

Spring 5-29-2019

Oxoborane Formation Turns on Formazanate-Based Photoluminescence

Ryan R. Maar

Nicholas A. Hoffman

Viktor N. Staroverov

Joe Gilroy
jgilroy5@uwo.ca

Follow this and additional works at: <https://ir.lib.uwo.ca/chempub>

 Part of the [Chemistry Commons](#)

Citation of this paper:

Maar, R.R.; Hoffman, N.A.; Staroverov, V.N.; Gilroy, J.B.* "Oxoborane Formation Turns on Formazanate-Based Photoluminescence" *Chemistry – A European Journal* **2019**, 25, 11015–11019.

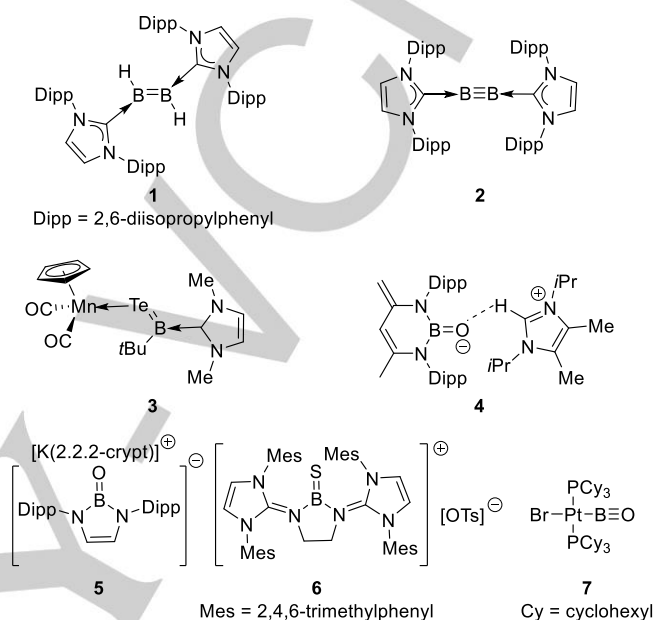
Oxoborane Formation Turns on Formazanate-Based Photoluminescence

Ryan R. Maar, Nicholas A. Hoffman, Viktor N. Staroverov, and Joe B. Gilroy*

Abstract: The synthesis of compounds containing multiple bonds to boron has challenged main-group chemists for decades. Despite significant progress, the possibility that the formation of such bonds can turn on photoluminescence has received minimal attention. We report an oxoborane (B=O) complex that is electronically stabilized by a formazanate ligand in the absence of significant steric bulk and, unlike the common BX_2 ($X = F, Cl$) formazanate adducts, exhibits intense photoluminescence. The latter property was rationalized through density-functional calculations which indicated that the B=O bond enhances photoluminescence by drastically reducing differences between the ligand's geometries in the ground and excited states. The title oxoborane compound was synthesized from an air- and moisture-stable BCl_2 formazanate complex and subsequently converted to a redox-active boroxine. Each of these species may also serve as a precursor to functional materials.

The discovery of main-group compounds with unusual structure and bonding is a major focus of interest in synthetic chemistry.^{[1],[2]} In this context, the preparation of stable compounds containing multiple bonds to boron presents a particular challenge due to the electron-deficient character and compactness of the valence orbitals of the B atom. To address these challenges, early efforts by the Berndt, Power, and Nöth groups utilized strong reducing agents to access anionic diboron species with boron-boron multiple bond character.^[3] More recent strategies of stabilizing double and triple bonds to boron have relied upon Lewis bases and/or sterically bulky substituents, as exemplified by compounds 1–7.^[4]

The first example of a neutral diborene, compound **1**, was reported by the Robinson group.^[4a] This molecule is stabilized by two sterically bulky and strongly σ -donating *N*-heterocyclic carbene ligands. Notable features of **1** include the short B=B bond of 1.560(18) Å and its *trans*-bent molecular structure. More recently, Braunschweig and co-workers^[4d] isolated diboryne **2**, the first example of a boron-boron triple bond. This molecule has an effectively linear geometry of the core atoms ($C \rightarrow B \equiv B \leftarrow C$) and a short B≡B bond length of 1.449(3) Å. Compounds with boron-chalcogen multiple bonds^{[5],[6]} have been isolated through the combination of strongly donating and sterically bulky ligands, as in compound **3**, which was prepared via insertion of elemental Te into a B=Mn bond.^[4f] The Cui group^[4c] reported the anionic β -diketiminato oxoborane complex **4**, stabilized through a hydrogen-bonding interaction, whereas the Aldridge group has recently reported an acid-free, anionic oxoborane **5**.^[7]

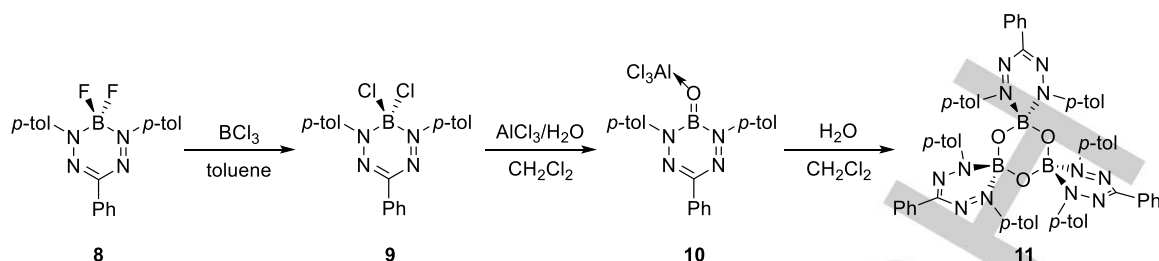


Thioxoborane **6** is the first cationic, electron-precise species containing a B=S bond.^[4e] The Braunschweig group has also prepared compound **7**,^[4b] which contains the first example of a boron-oxygen triple bond.

Apart from their intrinsic appeal from a fundamental perspective,^{[8],[9]} species with multiple bond character at boron show promise as reagents that allow one to carry out difficult chemical transformations, e.g., the functionalization of dinitrogen.^[10] Although compounds containing three-^[11] and four-^[12] coordinate boron centres have been utilized in optoelectronic materials design, molecules featuring multiple bonds involving boron have only recently emerged as viable candidates. So far, compounds with boron-boron multiple bonds have been shown to exhibit appreciable photoluminescence upon coordination to coinage metals,^[13] with the photophysics of the process implicating metal-borene or metal-boryne hybrid orbitals. Electron-rich diborenes have also been paired with π -accepting diarylboryls to produce molecules with near-infrared photoluminescence.^[14] While heterocycles containing BC^[15] or BN^[16] bonds with some π character are common, there appear to be no reports of photoluminescence induced by the formation of terminal double or triple bonds to boron. In this work, we demonstrate that the formation of the oxoborane (B=O) group transforms normally non-emissive boron triarylformazanate complexes into photoluminescent compounds. More generally, we suggest that combining boron multiple bonds and photoluminescent ligands may be an effective general approach for the production of photoluminescent materials.

Boron formazanate adducts **9–11** were prepared according to Scheme 1 (Figures S1–11). BF_2 formazanate **8**^[17] underwent halide exchange with BCl_3 to afford BCl_2 formazanate **9** as an

R.R. Maar, N.A. Hoffman, Prof. Dr. V. N. Staroverov, Prof. Dr. J. B. Gilroy
Department of Chemistry and The Centre for Advanced Materials and Biomaterials Research
The University of Western Ontario
1151 Richmond Street North, London, Ontario N6A 5B7 (Canada)
E-mail: joe.gilroy@uwo.ca



Scheme 1. Synthesis of boron formazanate adducts 9–11.

air- and moisture-stable, dark-purple solid in 78% yield after an aqueous workup. As a result of this transformation, the 1:2:1 triplet observed at -0.5 ppm in the ^{11}B NMR spectrum of complex **8** was replaced by a singlet at 2.4 ppm in the spectrum of **9**, confirming the presence of a four-coordinate boron centre. Complex **9** was surprisingly stable toward H_2O , but readily reacted with CH_3OH to give the $\text{B}(\text{OCH}_3)_2$ formazanate adduct (Figures S12–14) in 74% yield after column chromatography, probably because CH_3OH is slightly more nucleophilic than H_2O .^[18]

The stability of BCl_2 formazanate **9** allowed us to produce oxoborane formazanate complex **10** in a single synthetic step by mixing **9** with 1 equiv. of AlCl_3 and H_2O in CH_2Cl_2 solution. After stirring for 16 h, the solvent was removed and the residue was triturated with *n*-hexanes to afford a dark-purple microcrystalline solid in 94% crude yield (95% pure by ^1H NMR spectroscopy). Recrystallization from CH_2Cl_2 and hexanes produced compound **10** as dark-purple crystals in 15% yield. Complex **10** gave rise to a broad singlet in its ^{11}B NMR spectrum centred at 18.3 ppm that is consistent with other oxoboranes,^[4c, 6a, 6c, 7, 19] as well as a singlet in the ^{27}Al NMR spectrum ($\delta = 89.1$) corresponding to an oxygen-bound AlCl_3 fragment. The highly delocalized, nitrogen-rich backbone of formazanate ligands has been shown previously to stabilize radical anions based on B, Zn, and group-14 atoms.^[20] Similar electronic effects are likely responsible for the stability of compound **9** toward H_2O and for our ability to isolate oxoborane **10** in the absence of appreciable steric bulk.

Treatment of **10** with H_2O resulted in the formation of boroxine **11**, which is supported by three formazanate ligands, in 75% yield. The relatively simple ^1H and ^{13}C NMR spectra of boroxine **11** are indicative of C_{3v} symmetry and the ^{11}B NMR spectrum features a broad signal at -0.1 ppm.

Single crystals of compounds **9–11** were analyzed by X-ray diffraction, yielding their solid-state structures (Figure 1 and Tables S1–S3). The CN and NN bond lengths in complexes **9–11** ranged from $1.3379(19)$ to $1.351(3)$ Å and $1.3032(16)$ to $1.324(2)$ Å, respectively. These values are intermediate between the typical lengths of the respective single and double bond, which suggests that the π electrons of the formazanate backbone are delocalized.^[21] Compounds **9** and **11** feature four-coordinate, sp^3 -hybridized boron atoms that adopt distorted tetrahedral geometries and are displaced from the plane defined by the nitrogen atoms of the formazanate backbone(s) by an average distance of $0.434(2)$ Å (**9**) and $0.721(3)$ Å (**11**). In contrast, the boron atom in complex **10** deviates marginally from the ligand plane [$0.065(2)$ Å] and is sp^2 -hybridized, as evidenced by the sum of the bond angles about the boron atom

[$359.99(12)^\circ$]. Furthermore, the short boron oxygen bond [$1.3059(19)$ Å] in compound **10** is indicative of a BO double bond^[4c, 6a, 6c, 7, 19] and is significantly shorter than the average length of the single BO bonds in compound **11** [$1.412(3)$ Å].

The electrochemical properties of BF_2 formazanates such as **8** have been studied previously, revealing two sequential, generally reversible, one-electron reductions to their radical anion and dianion forms.^[17] Replacement of the fluorides with chlorides in complex **9** resulted in irreversible electrochemical reduction (Figure S15). In the case of boroxine **11**, the close proximity of the formazanate ligands gave rise to three distinct and reversible one-electron reduction waves ($E_{\text{red}1} = -1.49$ V; $E_{\text{red}2} = -1.74$ V; $E_{\text{red}3} = -1.95$ V relative to the Fc/Fc^+ redox couple) corresponding to the stepwise formation of ligand-based radical anions *en route* to a triradical trianion (Figures 2a and S16). This behaviour is attributed to coulombic interactions that resemble those observed during the electrochemical oxidation of cyclic ferrocenyl dimethylsilane trimers.^[22]

The electronic properties of compounds **9–11** were further investigated by analyzing their CH_2Cl_2 solutions using UV-vis absorption and photoluminescence spectroscopy (Figures 2b and S17 and Table 1). Complexes **9** and **11** are strongly

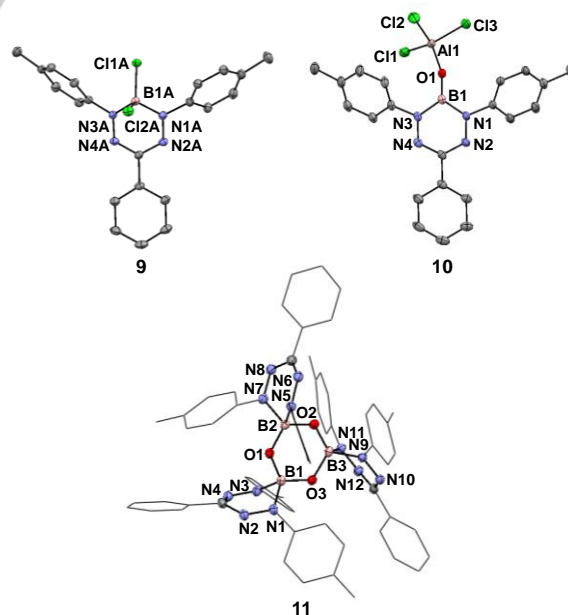


Figure 1. Solid-state structures of compounds 9–11. Anisotropic displacement ellipsoids are shown at the 50% probability level. Hydrogen atoms are omitted and the aryl-substituents in **11** are shown as wireframe for clarity.

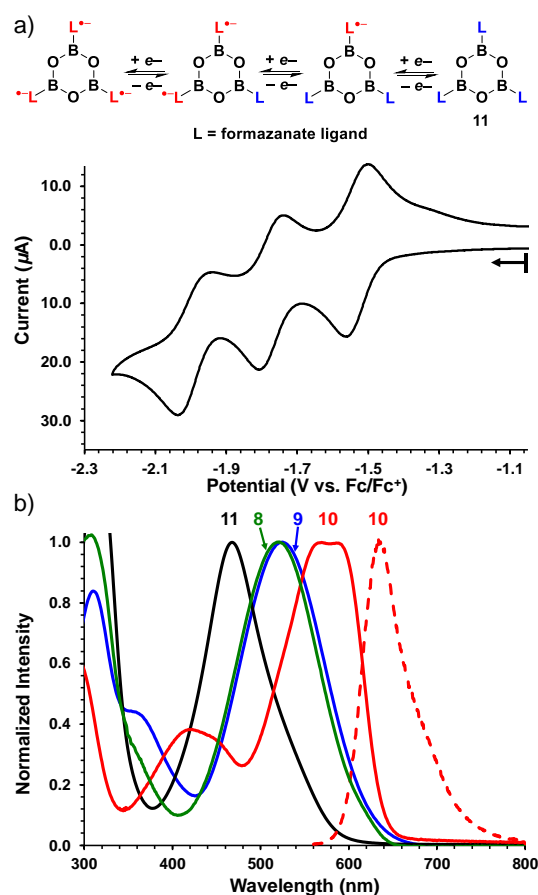


Figure 2. a) Cyclic voltammogram of a 1 mM CH_2Cl_2 solution of boroxine **11** containing 0.1 M $[\text{nBu}_4\text{N}][\text{PF}_6]$ as supporting electrolyte recorded at a scan rate of 100 mV s^{-1} . The arrow denotes the scan direction. b) Selected UV-vis absorption (solid lines) and photoluminescence (dashed line) spectra of 10^{-6} M dry and degassed CH_2Cl_2 solutions of formazanate adducts **8–11**. For additional absorption and photoluminescence spectra see Figure S17.

absorbing ($\epsilon = 14900\text{--}43800 \text{ M}^{-1} \text{ cm}^{-1}$) in the visible region of the electromagnetic spectrum and had broad absorption bands with maxima at 524 nm (**9**) and 468 nm (**11**), consistent with other four-coordinate boron adducts of formazanates, including compound **8** (520 nm, $\epsilon = 36600 \text{ M}^{-1} \text{ cm}^{-1}$).^[17, 25] In contrast, the absorption spectrum of oxoborane formazanate **10** contained two low-energy bands at 569 nm ($\epsilon = 36800 \text{ M}^{-1} \text{ cm}^{-1}$) and 586 nm ($\epsilon = 36700 \text{ M}^{-1} \text{ cm}^{-1}$) indicative of vibronic fine structure. The dominant orbital pair associated with the lowest energy absorption bands ($\pi \rightarrow \pi^*$) of **9** and **10** are the highest occupied molecular orbital (HOMO) and the lowest unoccupied molecular orbital (LUMO), as determined by time-dependent density-functional theory (TDDFT) calculations of electronic excitation energies (see below and Table 1). Based on related studies, we assume the same to be true for compounds **8** and **11**.^[25]

We and others have previously examined the origin of the weak photoluminescence of BF_2 triarylformazanates^{[26], [27]} compared to similar complexes of 3-nitro and 3-cyanoformazanates.^[25, 28] These studies have shown that non-radiative relaxation pathways involving rotations and/or vibrations of the carbon-bound aryl substituent^[26] and/or structural rearrangement upon photoexcitation^[27] lead to

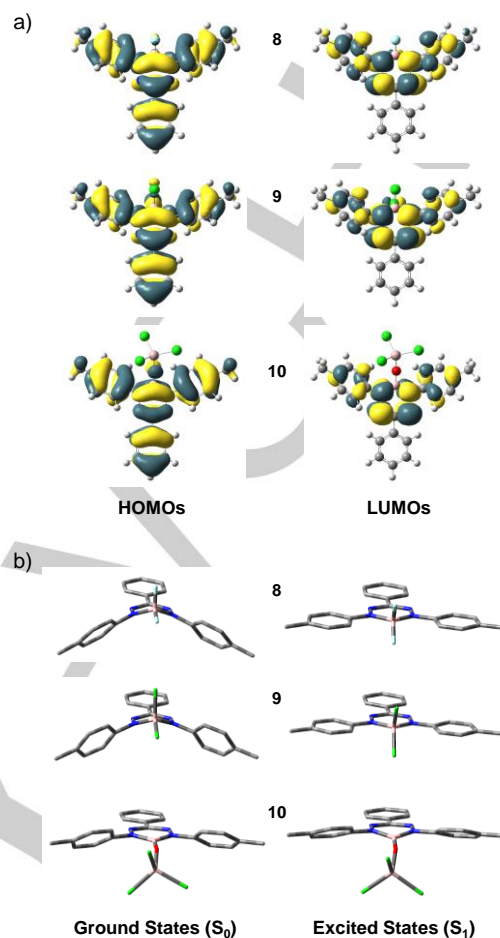


Figure 3. a) Frontier molecular orbitals and b) optimized geometries of boron triarylformazanates **8–10** calculated at the (TD)PBE1PBE/DGDZVP2 level of theory (CH_2Cl_2 solution). Hydrogen atoms in panel b) are omitted for clarity.

photoluminescence bands with low photoluminescence quantum yields (Φ_{PL}) and Stokes shifts ranging from 3070 to 3890 cm^{-1} . Consistent with those findings, complexes **8** ($\lambda_{\text{PL}} = 640 \text{ nm}$), **9** ($\lambda_{\text{PL}} = 698 \text{ nm}$), and **11** (no signal detected) were found to be essentially non-emissive in solution with Φ_{PL} values of less than 1% (Figure S17b). Unexpectedly, evaluation of the photoluminescence properties of oxoborane **10** ($\lambda_{\text{PL}} = 636 \text{ nm}$) revealed a much smaller Stokes shift of 1342 cm^{-1} and a >36-fold enhancement in photoluminescence intensity (Φ_{PL} of 36%). For comparison, the borylene and borynes mentioned earlier photoluminesce at wavelengths between 657 and 863 nm in toluene and their spectra were too weak to allow for quantum yields to be determined accurately.^[13–14] Only when these species were paired with coinage metals such as Cu and Ag was appreciable photoluminescence observed ($\lambda_{\text{PL}} 519\text{--}674 \text{ nm}$; $\Phi_{\text{PL}} 1\text{--}77\%$).^[13]

To understand the striking differences between oxoborane **10** and the chemically similar complexes **8** and **9**, we calculated and compared frontier molecular orbitals, ground- and excited-state molecular geometries, as well as the electronic excitation and PL spectra of the three compounds (using TDDFT for excited states). The calculations were carried out with the Gaussian program^[29] using the PBE1PBE functional,^[30] the

Table 1. Experimental and calculated spectroscopic properties of complexes **8–11** recorded in CH₂Cl₂ solution. The absorption and photoluminescence band maxima were calculated by linear-response TDDFT using the PBE1PBE/DGDZVP2 method and the polarizable continuum model of implicit solvation.

Compounds	Experiment					Theory		
	λ_{max} (nm)	ϵ (M ⁻¹ cm ⁻¹)	λ_{PL} (nm)	Φ_{PL} (%) ^[a]	ν_{ST} (cm ⁻¹)	λ_{max} (nm)	λ_{PL} (nm)	ν_{ST} (cm ⁻¹)
8	520	36600	640	< 1	3610	498	652	4743
9	524	14900	698	< 1	4757	512	716	5565
10 ^[b]	586	36700	636	36	1342	560	643	2305
	569	36800						
11	468	43800	–	0	–	–	–	–

^[a]Determined according to a published protocol^[23] using [Ru(bpy₃)](PF₆)₂ as a relative standard.^[24] ^[b]The experimental lowest-energy band has two maxima.

DGDZVP2 basis set, and the polarized continuum model of implicit solvation by CH₂Cl₂.

The HOMOs and LUMOs of boron triarylformazanates **8–10** (Figure 3a) show little variation and therefore cannot account for the dramatic difference between the photoluminescence properties of these compounds. The probable reason was revealed by examination of the optimized molecular geometries of **8–10** in their ground (S₀) and excited (S₁) electronic states. As shown in Figure 3b, electronic excitation of solvated molecules of **8** and **9** induces a drastic geometric change from strongly bent to almost perfectly planar structures. Such changes, characteristic of BF₂ formazanate complexes,^[27b, 31] are responsible for the relatively large Stokes shifts of **8** and **9** and for their weak photoluminescence. By contrast, oxoborane **10** undergoes little distortion upon electronic excitation. We presume the absence of significant geometry relaxation in **10** to be the key factor through which the B=O bond attenuates non-radiative decay pathways, reduces the Stokes shift, and turns on photoluminescence.

In conclusion, we have shown that the oxoborane formazanate complex **10** can be readily synthesized from complex **8** through air- and moisture-stable BCl₂ formazanate complex **9**. The product **10** is readily isolable and is stabilized not by steric bulk but by the electronic structure of the formazanate framework. Reaction of complex **10** with H₂O affords a boroxine **11**, which is supported by three redox-active formazanate ligands and can be converted electrochemically to a triradical trianion. Each of compounds **8–11** strongly absorbs visible light, but only the oxoborane formazanate complex **10** is photoluminescent with a Φ_{PL} of 36%. TDDFT calculations show that, unlike complexes **8** and **9**, the oxoborane **10** does not experience a large change in molecular geometry upon photoexcitation, which explains its relatively small Stokes shift and turn on photoluminescence behaviour.

These findings open up opportunities to exploit the structural rigidity imposed on formazanate complexes by B=O bonds to design photoluminescent materials. The proposed approach can in principle be expanded by altering the identity of the main-group element (E) bonded to boron or the ligand framework. In a broader sense, exploration of photoluminescent compounds with B=E and B≡E bonds would strengthen the link between current trends in main-group chemistry and optoelectronic materials design and may lead to the creation of a wide range of unprecedented molecular materials.

Acknowledgements

This work was supported by the Natural Sciences and Engineering Research Council (NSERC) of Canada (V.N.S: DG,

RGPIN-2015-04814; J.B.G.: DG, RGPIN-2018-04240, R.R.M.: CGS-D Scholarship), the Ontario Ministry of Research and Innovation (J.B.G.: ERA, ER-14-10-147), and the Canadian Foundation for Innovation (J.B.G.: JELF, 33977).

Keywords: Oxoboranes • Boron multiple bonds • Formazanate ligands • Turn on photoluminescence • X-ray crystallography

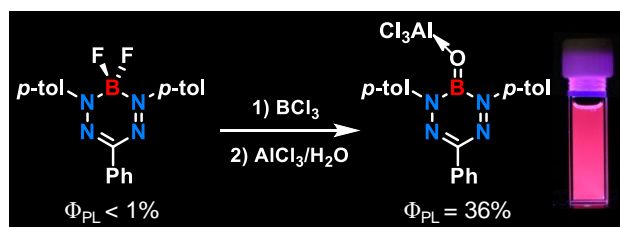
- Selected examples: a) D. Franz, T. Szilvási, E. Irran, S. Inoue, *Nat. Commun.* **2015**, *6*, 10037; b) A. Rit, J. Campos, H. Niu, S. Aldridge, *Nat. Chem.* **2016**, *8*, 1022–1026; c) M. M. Hansmann, R. Jazzar, G. Bertrand, *J. Am. Chem. Soc.* **2016**, *138*, 8356–8359; d) P. Bag, A. Porzelt, P. J. Altmann, S. Inoue, *J. Am. Chem. Soc.* **2017**, *139*, 14384–14387; e) B. Su, K. Ota, K. Xu, H. Hirao, R. Kinjo, *J. Am. Chem. Soc.* **2018**, *140*, 11921–11925; f) T. Wang, C. G. Daniliuc, C. Mück-Lichtenfeld, G. Kehr, G. Erker, *J. Am. Chem. Soc.* **2018**, *140*, 3635–3643; g) M. J. Drance, J. D. Sears, A. M. Mrse, C. E. Moore, A. L. Rheingold, M. L. Neidig, J. S. Figueroa, *Science* **2019**, *363*, 1203–1205; h) W. Lu, Y. Li, R. Kinjo, *J. Am. Chem. Soc.* **2019**, *141*, 5164–5168; i) J. R. Gaffen, J. N. Bentley, L. C. Torres, C. Chu, T. Baumgartner, C. B. Caputo, *Chem* **2019**, DOI: 10.1016/j.chempr.2019.03.022.
- Reviews: a) P. P. Power, *Chem. Rev.* **1999**, *99*, 3463–3504; b) Y. Wang, G. H. Robinson, *Chem. Commun.* **2009**, 5201–5213; c) R. C. Fischer, P. P. Power, *Chem. Rev.* **2010**, *110*, 3877–3923.
- a) H. Klusik, A. Berndt, *Angew. Chem. Int. Ed.* **1981**, *20*, 870–871; b) A. Moezzi, M. M. Olmstead, P. P. Power, *J. Am. Chem. Soc.* **1992**, *114*, 2715–2717; c) W. J. Grigsby, P. P. Power, *Chem. Commun.* **1996**, 2235–2236; d) H. Nöth, J. Knizek, W. Ponikvar, *Eur. J. Inorg. Chem.* **1999**, 1999, 1931–1937.
- a) Y. Wang, B. Quillian, P. Wei, C. S. Wannere, Y. Xie, R. B. King, H. F. Schaefer, P. v. R. Schleyer, G. H. Robinson, *J. Am. Chem. Soc.* **2007**, *129*, 12412–12413; b) H. Braunschweig, K. Radacki, A. Schneider, *Science* **2010**, *328*, 345–347; c) Y. Wang, H. Hu, J. Zhang, C. Cui, *Angew. Chem. Int. Ed.* **2011**, *50*, 2816–2819; d) H. Braunschweig, R. D. Dewhurst, K. Hammond, J. Mies, K. Radacki, A. Vargas, *Science* **2012**, *336*, 1420–1422; e) D. Franz, E. Irran, S. Inoue, *Angew. Chem. Int. Ed.* **2014**, *53*, 14264–14268; f) S. Liu, M.-A. Légaré, D. Auerhammer, A. Hofmann, H. Braunschweig, *Angew. Chem. Int. Ed.* **2017**, *56*, 15760–15763.
- D. Franz, S. Inoue, *Dalton Trans.* **2016**, *45*, 9385–9397.
- a) D. Vidovic, J. A. Moore, J. N. Jones, A. H. Cowley, *J. Am. Chem. Soc.* **2005**, *127*, 4566–4567; b) H. Wang, J. Zhang, H. Hu, C. Cui, *J. Am. Chem. Soc.* **2010**, *132*, 10998–10999; c) Y. K. Loh, C. C. Chong, R. Ganguly, Y. Li, D. Vidovic, R. Kinjo, *Chem. Commun.* **2014**, *50*, 8561–8564.
- Y. K. Loh, K. Porteous, M. Á. Fuentes, D. C. H. Do, J. Hicks, S. Aldridge, *J. Am. Chem. Soc.* **2019**, *141*, 8073–8077.
- Reviews: a) H. Braunschweig, R. D. Dewhurst, *Organometallics* **2014**, *33*, 6271–6277; b) M. Arrowsmith, H. Braunschweig, T. E. Stennett, *Angew. Chem. Int. Ed.* **2017**, *56*, 96–115.
- Selected examples: a) T. Kaese, A. Hübner, M. Bolte, H.-W. Lerner, M. Wagner, *J. Am. Chem. Soc.* **2016**, *138*, 6224–6233; b) W. Lu, Y. Li, R. Ganguly, R. Kinjo, *J. Am. Chem. Soc.* **2017**, *139*, 5047–5050; c) W. Lu,

- Y. X. Li, R. Ganguly, R. Kinjo, *Angew. Chem. Int. Ed.* **2017**, *56*, 9829–9832; d) S. Morisako, R. Shang, Y. Yamamoto, H. Matsui, M. Nakano, *Angew. Chem. Int. Ed.* **2017**, *56*, 15234–15240; e) W. Lu, Y. X. Li, R. Ganguly, R. Kinjo, *J. Am. Chem. Soc.* **2018**, *140*, 1255–1258; f) T. E. Stennett, J. D. Mattock, I. Vollert, A. Vargas, H. Braunschweig, *Angew. Chem. Int. Ed.* **2018**, *57*, 4098–4102.
- [10] a) M.-A. Légaré, G. Bélanger-Chabot, R. D. Dewhurst, E. Welz, I. Krummenacher, B. Engels, H. Braunschweig, *Science* **2018**, *359*, 896–900; b) M.-A. Légaré, M. Rang, G. Bélanger-Chabot, J. I. Schweizer, I. Krummenacher, R. Bertermann, M. Arrowsmith, M. C. Holthausen, H. Braunschweig, *Science* **2019**, *363*, 1329–1332.
- [11] Selected reviews: a) C. D. Entwistle, T. B. Marder, *Chem. Mater.* **2004**, *16*, 4574–4585; b) Y. Ren, F. Jäkle, *Dalton Trans.* **2016**, *45*, 13996–14007; c) L. Ji, S. Griesbeck, T. B. Marder, *Chem. Sci.* **2017**, *8*, 846–863.
- [12] Selected reviews: a) A. Loudet, K. Burgess, *Chem. Rev.* **2007**, *107*, 4891–4932; b) Y.-L. Rao, S. Wang, *Inorg. Chem.* **2011**, *50*, 12263–12274; c) D. Frath, J. Massue, G. Ulrich, R. Ziessel, *Angew. Chem. Int. Ed.* **2014**, *53*, 2290–2310.
- [13] a) P. Bissinger, A. Steffen, A. Vargas, R. D. Dewhurst, A. Damme, H. Braunschweig, *Angew. Chem. Int. Ed.* **2015**, *54*, 4362–4366; b) H. Braunschweig, T. Dellermann, R. D. Dewhurst, B. Hupp, T. Kramer, J. D. Mattock, J. Mies, A. K. Phukan, A. Steffen, A. Vargas, *J. Am. Chem. Soc.* **2017**, *139*, 4887–4893.
- [14] T. E. Stennett, P. Bissinger, S. Griesbeck, S. Ullrich, I. Krummenacher, M. Auth, A. Sperlich, M. Stolte, K. Radacki, C.-J. Yao, F. Würthner, A. Steffen, T. B. Marder, H. Braunschweig, *Angew. Chem. Int. Ed.* **2019**, *58*, 6449–6454.
- [15] Selected reviews: a) A. Escande, M. J. Ingleson, *Chem. Commun.* **2015**, *51*, 6257–6274; b) E. von Grothuss, A. John, T. Kaese, M. Wagner, *Asian J. Org. Chem.* **2018**, *7*, 37–53; c) A. Wakamiya, *Main Group Strategies towards Functional Hybrid Materials* (Eds.: T. Baumgartner, F. Jäkle), **2018**, p. 1–26; d) M. Hirai, N. Tanaka, M. Sakai, S. Yamaguchi, *Chem. Rev.* **2019**, DOI: 10.1021/acs.chemrev.8b00637.
- [16] Selected reviews: a) M. J. D. Bosdet, W. E. Piers, *Can. J. Chem.* **2009**, *87*, 8–29; b) P. G. Campbell, A. J. V. Marwitz, S.-Y. Liu, *Angew. Chem. Int. Ed.* **2012**, *51*, 6074–6092; c) X.-Y. Wang, J.-Y. Wang, J. Pei, *Chem. Eur. J.* **2015**, *21*, 3528–3539; d) M. M. Morgan, W. E. Piers, *Dalton Trans.* **2016**, *45*, 5920–5924; e) Z. X. Giustra, S.-Y. Liu, *J. Am. Chem. Soc.* **2018**, *140*, 1184–1194.
- [17] S. M. Barbon, J. T. Price, P. A. Reinkeluers, J. B. Gilroy, *Inorg. Chem.* **2014**, *53*, 10585–10593.
- [18] S. Minegishi, S. Kobayashi, H. Mayr, *J. Am. Chem. Soc.* **2004**, *126*, 5174–5181.
- [19] A. K. Swarnakar, C. Hering-Junghans, M. J. Ferguson, R. McDonald, E. Rivard, *Chem. Eur. J.* **2017**, *23*, 8628–8631.
- [20] a) M.-C. Chang, T. Dann, D. P. Day, M. Lutz, G. G. Wildgoose, E. Otten, *Angew. Chem. Int. Ed.* **2014**, *53*, 4118–4122; b) R. Mondol, D. A. Snoeken, M.-C. Chang, E. Otten, *Chem. Commun.* **2017**, *53*, 513–516; c) R. R. Maar, S. D. Catingan, V. N. Staroverov, J. B. Gilroy, *Angew. Chem. Int. Ed.* **2018**, *57*, 9870–9874.
- [21] J. R. Rumble, *CRC Handbook of Chemistry and Physics, 98th ed.*, CRC Press/Taylor and Francis, Boca Raton, FL.
- [22] D. E. Herbert, J. B. Gilroy, W. Y. Chan, L. Chabanne, A. Staubitz, A. J. Lough, I. Manners, *J. Am. Chem. Soc.* **2009**, *131*, 14958–14968.
- [23] S. Fery-Forgues, D. Lavabre, *J. Chem. Educ.* **1999**, *76*, 1260–1264.
- [24] K. Suzuki, A. Kobayashi, S. Kaneko, K. Takehira, T. Yoshihara, H. Ishida, Y. Shiina, S. Oishi, S. Tobita, *Phys. Chem. Chem. Phys.* **2009**, *11*, 9850–9860.
- [25] S. M. Barbon, V. N. Staroverov, J. B. Gilroy, *J. Org. Chem.* **2015**, *80*, 5226–5235.
- [26] S. M. Barbon, J. V. Buddingh, R. R. Maar, J. B. Gilroy, *Inorg. Chem.* **2017**, *56*, 12003–12011.
- [27] a) M.-C. Chang, A. Chantzis, D. Jacquemin, E. Otten, *Dalton Trans.* **2016**, *45*, 9477–9484; b) M. Hesari, S. M. Barbon, R. B. Mendes, V. N. Staroverov, Z. Ding, J. B. Gilroy, *J. Phys. Chem. C* **2018**, *122*, 1258–1266.
- [28] S. M. Barbon, P. A. Reinkeluers, J. T. Price, V. N. Staroverov, J. B. Gilroy, *Chem. Eur. J.* **2014**, *20*, 11340–11344.
- [29] M. J. Frisch, G. W. Trucks, H. B. Schlegel, G. E. Scuseria, M. A. Robb, J. R. Cheeseman, G. Scalmani, V. Barone, G. A. Petersson, H. Nakatsuji et. al. Gaussian Development Version, Revision I.13; Gaussian, Inc.: Wallingford, CT, 2016.
- [30] a) M. Ernzerhof, G. E. Scuseria, *J. Chem. Phys.* **1999**, *110*, 5029–5036; b) C. Adamo, G. E. Scuseria, V. Barone, *J. Chem. Phys.* **1999**, *111*, 2889–2899.
- [31] A. D. Laurent, E. Otten, B. Le Guennic, D. Jacquemin, *J. Mol. Model.* **2016**, *22*, 263.

Entry for the Table of Contents

Layout 2:

COMMUNICATION



Ryan R. Maar, Nicholas A. Hoffman,
Viktor N. Staroverov, Joe B. Gilroy*

Page No. – Page No.

**Oxoborane Formation Turns on
Formazanate-Based
Photoluminescence**

Conversion of non-emissive BX_2 ($X = F$ or Cl) formazanate adducts to the corresponding oxoborane ($B=O$) complex turns on bright photoluminescence. Density-functional theory calculations suggest that this occurs because the $B=O$ complex undergoes a much smaller geometric relaxation upon photoexcitation than do the BX_2 adducts.